

Theoretical Study of the Spinel Structure of CuCr_2O_4 in the Tetragonal Phase Using Density Functional Theory

Radia Bencheikh, Karima Belakroum

*Université Kasdi Merbah-Ouargla, Faculté des Mathématiques et des Sciences de la Matière,
Département de Physique, Route de Ghardaïa 30000, Alegria*

(Received 03 August 2022; revised manuscript received 24 October 2022; published online 28 October 2022)

We report a detailed theoretical study of ternary spinel oxides CuCr_2O_4 with tetragonal $I4_1/amd$ structures by means of density functional theory (DFT). The calculations were performed using two approximations to DFT, namely, the local density approximation (LDA) and the generalized gradient approximation (GGA), both in the spin-polarized version. For LDA, we used the Ceperley-Alder exchange-correlation potential, whereas for the GGA calculations, we used the Perdew-Burke-Ernzerhof (PBE) scheme. We optimized the crystal structures using a pseudopotential plane wave method and analyzed on the basis of the density of states (DOS), partial density of states (PDOS), and electronic band structure. Indeed, it is a useful method to predict the crystal structures of CuCr_2O_4 . The PDOS of Cu, Cr, and O revealed that the Cr cation is the dominant source to study the magnetic properties of CuCr_2O_4 . Spin polarization calculations performed for CuCr_2O_4 , and DOS show that there is a large spin splitting between the spin up down channels near the Fermi level, confirming p - d hybridization. The theoretical calculated magnetic moment is slightly higher than the experimental results. It was concluded that the optimized GGA lattice parameter agrees much better with the experimental findings than the LDA one. The valence and conduction bands overlapped each other at the Fermi level, indicating the metallic nature of CuCr_2O_4 . The charge density difference maps indicate that Cu–Cr bonds are stronger than Cu–O. The obtained results were compared with experimental values and a good agreement with them was found. The results of the present study could be used in a future analysis of the thermodynamical, optical and elastic properties of this compound.

Keywords: CuCr_2O_4 , Spinel structure, Density functional theory (DFT), Electronic band structure, Magnetic properties.

DOI: [10.21272/jnep.14\(5\).05030](https://doi.org/10.21272/jnep.14(5).05030)

PACS numbers: 71.20. – b, 78.20.Ci

1. INTRODUCTION

Many chalcogenide spinels have the general formula AB_2X_4 , tetrahedral A cations are divalent, octahedral B cations are trivalent, and X anions are divalent. The cations occupy 1/8 of the tetrahedral (A) and 1/2 of the octahedral (B) voids within the face-centered cubic (fcc) lattice formed by the X anions [1, 2] corresponding to the space group $\text{FD}\bar{3}m$. This family of compounds exhibits a variety of fascinating physical properties, and they have been used in a wide range of applications. It is an emerging technological material with a variety of promising applications in various fields [2]. Several studies on ACr_2O_4 spinel oxides have been reported in literature [1, 3, 4]. Ternary normal spinels with stoichiometric composition $\text{A}^{2+}\text{Cr}^{3+}_2\text{O}_4$ are typical candidates for studying the magnetic properties of frustrated systems [2, 5–8]. The cations of Cr^{3+} at the B site are octahedrally coordinated and form a pyrochlore-type lattice, one of the strongest contenders of geometric frustration in three dimensions [8], while the A-site cations are tetrahedrally coordinated, constituting a diamond-type lattice with tetrahedral oxygen environment [8–10]. The presence of magnetic moment and orbital degeneracy on the A-site ions can change the magnetic and structural properties [11]. On the other hand, frustration is released as a result of the structural phase transition, from cubic to lower structural symmetry [4, 12, 13]. Copper chromite CuCr_2O_4 is an insulating ferrimagnet and crystallizes at room temperature (above 320 K) in a tetragonal distorted spinel in the $I4_1/amd$ space group, due to cooperative Jahn-Teller ordering, the lattice parameters are

$a = 8.5 \text{ \AA}$ and $c = 7.8 \text{ \AA}$. Above 853°K [4, 14, 15] its structure is a normal cubic spinel with the space group $\text{Fd}\bar{3}m$, the lattice parameter is $a = 8.3543(3) \text{ \AA}$ [16, 17]. Furthermore, the Jahn-Teller distortion is suppressed above 870 K [17], whereas cooling leads to a coupled magnetostructural transition into a ferrimagnetic orthorhombic phase at 135 K [18, 19]. This significant diversity in physical properties of the frustrated spinel compound CuCr_2O_4 prompted us to investigate the electronic band structure, energy band gap, density of states in the tetragonal phase by using DFT calculations.

2. COMPUTATIONAL DETAILS

The calculations have been performed using Density Functional Theory (DFT) as implemented in the Spanish Initiative for Electronic Simulations with Thousands of Atoms code Siesta-3-2 [20]. Both the generalized gradient approximation (GGA-PBE) [21] and local density approximation (LDA-CA) [22] methods were selected to treat the exchange-correlation interaction. The double- ζ plus polarization (DZP) basis sets are chosen to represent the atomic orbitals of the different types of atoms included in this study [22]. The valence configurations Cu ($3d^{10}4s^1$), Cr ($3d^5 4s^1$) and O ($2s^2 2p^4$) were chosen. The kinetic energy cut-off is optimized for the tetragonal phase up to 100 Ry. For the all-electron variant in the case of the tetragonal phase, the cut-off parameter is calculated from the dimensional number $\text{RMT}_{\min} \times K_{\max}$, where RMT_{\min} is the smallest Muffin-Tin sphere and K_{\max} is the largest reciprocal lattice vector used to represent the all-electron wave function. The k -point mesh

in the first Brillouin zone (BZ) for the tetragonal phase is optimized to $(9 \times 9 \times 3)$ 122 k -point. These values were obtained by ensuring total energy convergence as it is shown in Fig. 1 and Fig. 2.

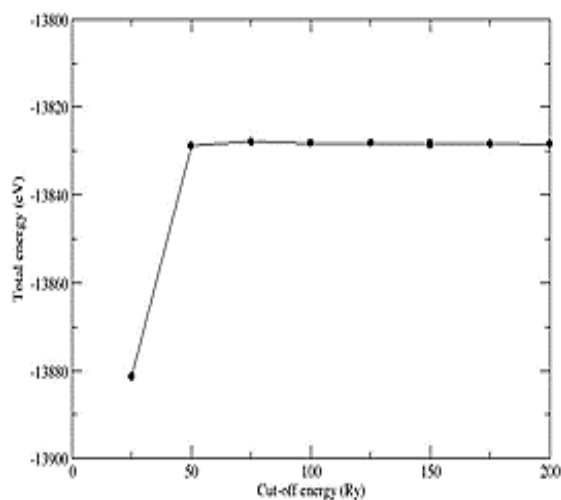


Fig. 1 – Convergence test with respect to the energy cut off

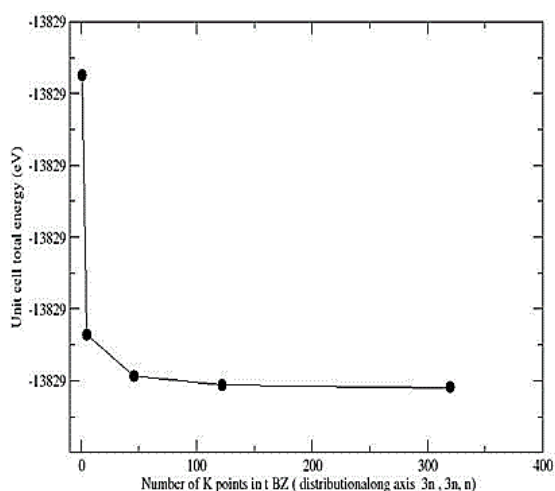


Fig. 2 – Convergence test with respect to k -point

3. RESULTS AND DISCUSSION

In this section, we present the theoretical study of the structural, electronic and magnetic properties of the tetragonal phase of frustrated spinel oxide CuCr_2O_4 .

3.1 Structural Properties

Since the structure relates closely to the electronic and magnetic properties, we first optimized the unit-cell parameters of CuCr_2O_4 , and then calculated the other properties. The calculations were performed using the local density approximation (LDA) and the generalized gradient approximation (GGA), both in the spin-polarized version. For LDA, we used the Ceperley-Alder exchange correlation potential [22], whereas for the GGA calculations, we used the Perdew-Burke-Ernzerhof (PBE) scheme [21]. CuCr_2O_4 has a normal spinel structure, where Cu, Cr and O represent a divalent cation, a trivalent cation, and a divalent anion, respectively. At room temperature, the normal oxide spinel CuCr_2O_4 is

tetragonally distorted and crystallizes in $I4_1/amd$ (No 141) [23] space group due to cooperative Jahn-Teller ordering driven by orbital degeneracy of tetrahedral Cu^{2+} (t_2^5) [19]. The conventional and primitive unit cell of this spinel is shown in Fig. 3 (XCrySDen graphic software, which is a program for visualizing crystalline and molecular structures, was used [24]).

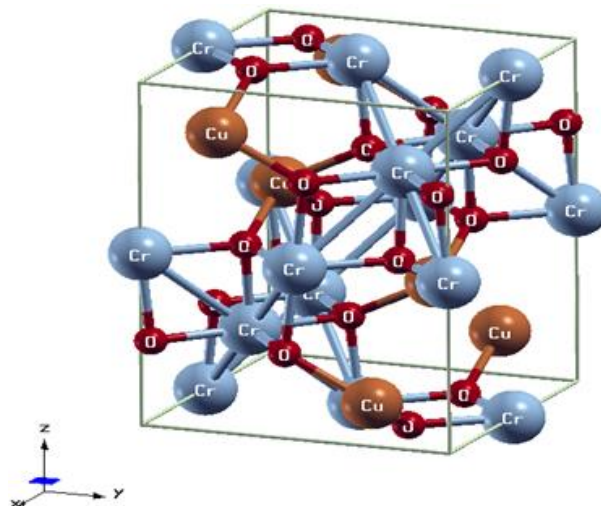


Fig. 3 – Tetragonal crystal structure of CuCr_2O_4 spinel

In order to confirm the stability of spinel CuCr_2O_4 and the precision of our calculations, the lattice parameters and cell volume are given in Table 1 with available experimental values for comparison. Our obtained results are in good agreement with those of other works [25, 26, 27]. According to the results shown in Table 1, it is obvious that the calculated and experimental results differ slightly due to the temperature dependence of the cell parameters. It is well known that the GGA lattice parameter a slightly overestimates the experimental value, while the LDA value is clearly smaller than the experimental one [28].

Table 1 – Calculated lattice constants (a , b and c in Å, V in Å³) of CuCr_2O_4

Space group	$I4_1/amd$	
Compound	CuCr_2O_4	
Lattice constant present work	GGA-PBE	LDA-CA
	$a = 6.11 \text{ \AA}$, $b = 6.11 \text{ \AA}$, $c = 7.83 \text{ \AA}$, $V = 292310(0) \text{ \AA}^3$	$a = 6.09 \text{ \AA}$, $b = 6.09 \text{ \AA}$, $c = 7.81 \text{ \AA}$, $V = 282.943(3) \text{ \AA}^3$
Exp	$a = 6.03277(1) \text{ \AA}^a$, $b = 6.3277(1) \text{ \AA}^a$, $c = 7.78128(1) \text{ \AA}^a$, $V = 283.243(4) \text{ \AA}^3$, $a = 6.0341(4) \text{ \AA}^b$, $b = 6.0341(4) \text{ \AA}^b$, $c = 7.7888(6) \text{ \AA}^b$, $V = 283.603(4) \text{ \AA}^{3b}$, $a = 6.038(2) \text{ \AA}^c$, $b = 6.038(2) \text{ \AA}^c$, $c = 7.784(5) \text{ \AA}^c$, $V = 283.410(4) \text{ \AA}^3$, $a = 6.03052(14) \text{ \AA}^d$, $b = 6.03052(14) \text{ \AA}^d$, $c = 7.78230(21) \text{ \AA}^d$, $V = 283.0202(4) \text{ \AA}^3$	

^aRef.[19]-Exp, ^bRef. [17]-Exp, ^cRef. [7]-Exp, ^dRef. [15]-Exp

This feature is also observed in several similar systems in other simulation works [25, 26, 29]. The computed results reveal that LDA can give more accurate data than GGA for the studied oxide system and are in good agreement with experimental measurements [27, 29].

3.2 Electronic Properties

The spin-polarized band structure of the tetragonal phase is calculated with GGA-PBE and LDA-CA approximations at 0 K. The results are illustrated in Fig. 4 and Fig. 5, respectively. The band structure is calculated along the directions of higher symmetries in the first Brillouin zone for an energy range from -20 to 4 eV. The line at 0 K indicates the Fermi level. It is clearly seen that from the band structure patterns that there is an overlap between the valence and conduction bands at the Fermi level; also, the maximum of the valence band is above the Fermi level. Indeed, the crossings of bands with the Fermi level are not the same in two approximations. This can be attributed to the fact that $3d$ orbitals of Cu, that form most of the top of the valence band, are not well localized [30]. Moreover, another significant feature of the band structures in Fig. 4 and Fig. 5 is the different positions of the valence bands (at Γ), where in LDA they shift towards higher energies at the top of the valence band and towards lower energies at the bottom of the valence band. All this indicates a slight increase in bandwidth as a consequence of the reduced lattice parameter. We note from Fig. 4 and Fig. 5 that two curves of DOS calculated with GGA-PBE and LDA-CA have the same overall shape; the overlapping of the valence and conduction bands at the Fermi level in the two directions (Z-r) indicates that CuCr_2O_4 has a metallic nature with evidence of zero band gap. Our results within GGA-PBE approximation are closer to the experimental one.

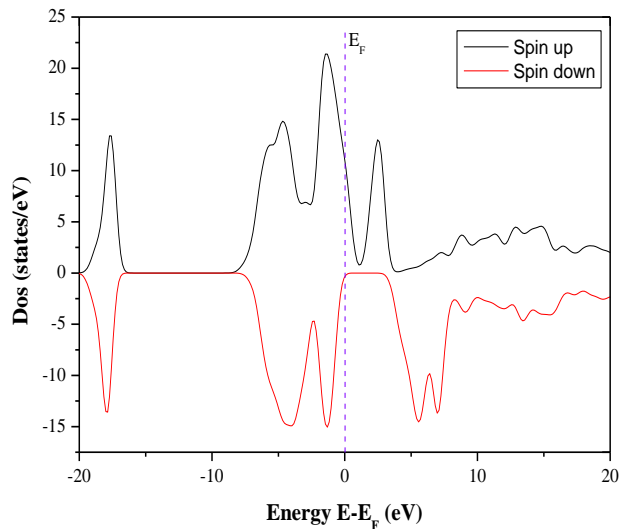


Fig. 4 – Band structure of CuCr_2O_4 within GGA-PBE

3.3 Electronic and Magnetic Properties

The total density of states (TDOS) for the CuCr_2O_4 compound is analyzed using GGA-PBE and LDA-CA, as shown in Fig. 6 and Fig. 7, respectively. Fig. 8 shows the partial density of states (PDOS) for CuCr_2O_4 analyzed using GGA-PBE. The Fermi level position is taken as a reference point to determine DOS and PDOS. We note from Fig. 6 and Fig. 7 that TDOS calculated with GGA-PBE and LDA-CA approximations of CuCr_2O_4 is divided into four-spin regions: spin up and spin down.

Spin polarization calculations are performed on the CuCr_2O_4 and DOS show there exists large spin splitting

between the spin up down channels near the Fermi level confirm p - d hybridization [31].

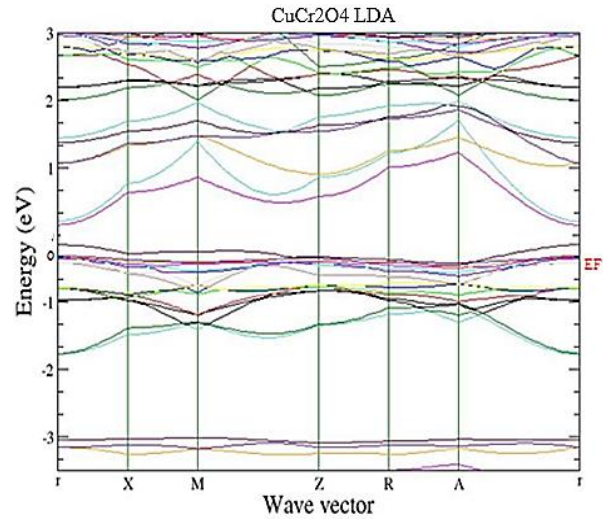


Fig. 5 – Band structure of CuCr_2O_4 within LDA-CA

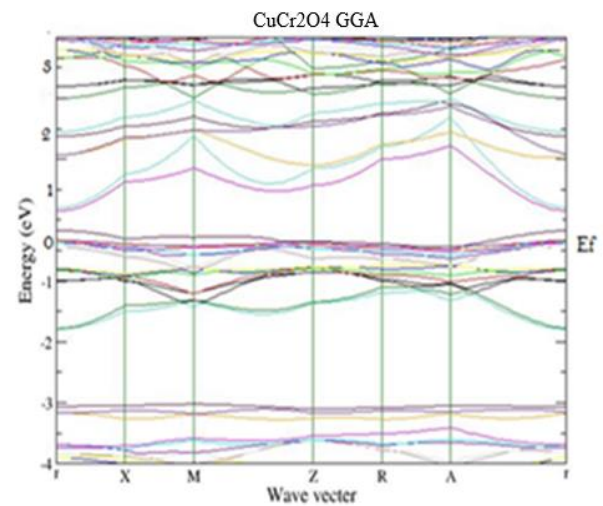


Fig. 6 – TDOS of CuCr_2O_4 calculated by DFT within GGA-PBE, the Fermi level E_F is indicated by the vertical line

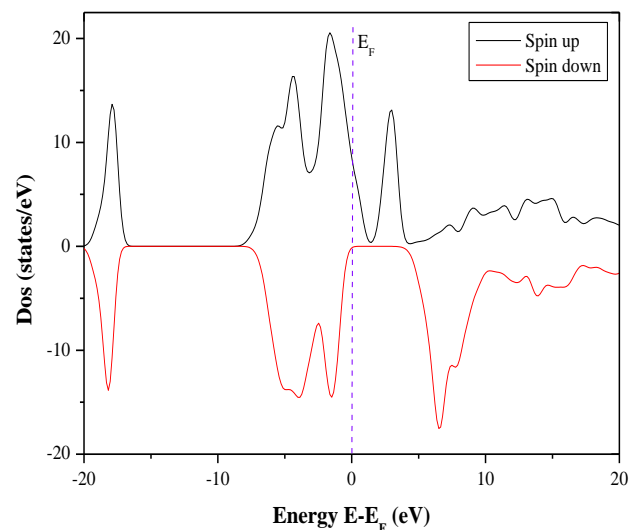


Fig. 7 – TDOS of CuCr_2O_4 calculated by DFT within LDA-CA, the Fermi level E_F is indicated by the vertical line

From Fig. 6 it is seen that the first is a sharp peak located at a round -3.7 eV to the Fermi level. The second region located in the range from -8.6 to -3.7 eV manifests hybridization of Cu $3d$ orbitals as well as hybridization of Cr orbitals. The third is lying in the range from 16.86 to 19.9 eV, arising from Cu $4s$ and Cr $3d$ orbitals, and the fourth peak is at 3.2 eV due to the O $2p$ contribution.

From Fig. 6 and Fig. 7 we note that two TDOS curves of CuCr_2O_4 with LDA-CA and GGA-PBE are almost identical, resulting from the same previous contribution of the same atoms and orbitals. However, we note that the highest value of TDOS for CuCr_2O_4 in two approximations was recorded for LDA-CA. On the other hand, in order to understand the magnetic properties of CuCr_2O_4 , the PDOS is calculated and explained; for this we need to know at first PDOS for Cu, Cr and O contributions.

From Fig. 8, the PDOS spectra of spin channels arise mainly from the filled Cu $3d$ and Cr $3d$ orbitals, adding O $2p$ orbitals to the light contribution. The second region for spin up arises mainly from Cu $3d$ and Cr $3d$ orbitals in the range from -3.5 to -8 eV. The third peak is located from -20 to -17 eV, it arises mainly from Cu $4s$ orbitals. In addition, the fourth peak at 2.1 eV mainly arises from O $2p$ orbital. The band gap around the Fermi level results from Cu $3d$ orbitals for spin up and spin down. A higher DOS value at 10.2 states/eV manifests hybridization of Cu $3d$ orbitals, as well as hybridization of Cr $3d$ as seen in Fig. 8.

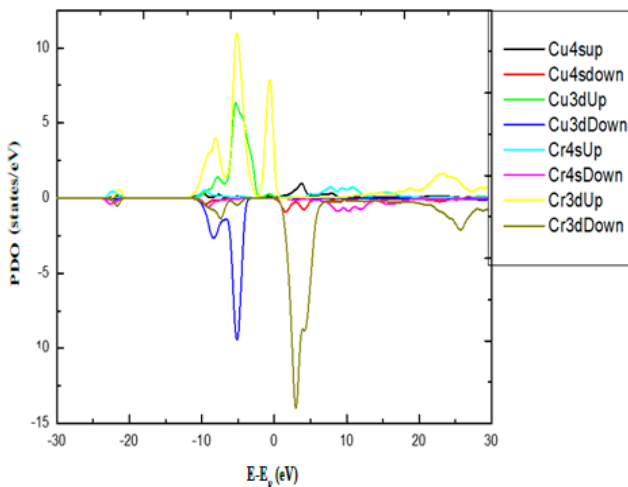


Fig. 8 – PDOS of the tetragonal structure of CuCr_2O_4 within GGA-PBE

From Fig. 6 and Fig. 7, we note that DOS is zero for spin up and the weak contribution is mainly from $2p$ orbital (spin down); for this reason, curves showing PDOS of the O atom are not plotted. Fig. 9 and Fig. 10 show PDOS for the Cr atom with GGA-PBE (a) and LDA-CA (b), and PDOS for the Cu atom with GGA-PBE (a) and LDA-CA (b), respectively.

It appears from Fig. 9a that PDOS curves of the Cr atom with GGA-PBE are divided into three spin regions, lying in the range from -12 eV to E_F . The highest peak is at 9.7 states/eV, in addition Cr $3d$ electrons provide PDOS of -5.7 states/eV. The third value appears at 2.3 states/eV and a band gap appears within the $3d$

down orbital beyond the Fermi level. As for spin down, we find one peak at 2.2 eV, where the value of PDOS reaches 5.5 states/eV. From Fig. 9b, we notice that there are three higher spin peaks arising from the $3d$ up orbital. These peaks lie within the energy range from -12.1 eV to the Fermi level. The highest peak is at 9.71 states/eV. The Cr $3d$ electrons provide PDOS of -6 states/eV. The third value appears at 2.4 states/eV, a band gap appears within the $3d$ down orbital after the Fermi level, and for the lowest spin we find two peaks, the first at 2.3 eV, providing -12 states/eV, while the second at 3 eV, the PDOS value reaches -11 states/eV.

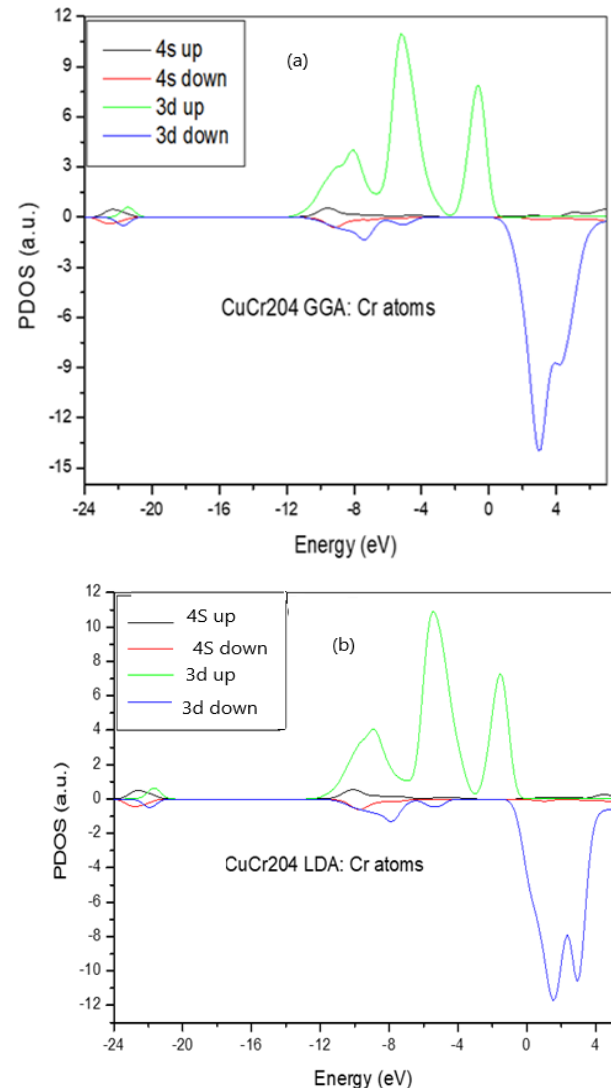


Fig. 9 – PDOS of the Cr atom calculated with (a) LDA-CA and (b) LDA

From Fig. 10, it appears that two PDOS curves of the Cu atom calculated using GGA-PBE and LDA-CA have the same overall shape. Therefore, we can see a band gap formed by the $3d$ up orbital at -3 eV, a higher value of PDOS reaches 6 states/eV. There is a weak contribution of $4s$ up and another peak found at -4.2 eV, formed by a weak contribution of $3d$ down.

It is noticeable from Fig. 10b that PDOS of Cu atoms calculated using LDA-CA is formed by a band gap at -5 eV, mainly due to $3d$ up contribution, the value of

PDOS reaches 7 states/eV, and a very low contribution of 4s up. In addition, there is another peak at -5 eV due to the contribution of 3d down.

The total magnetic moment of atoms calculated from GGA-PBE and LDA-CA is presented in Table 3.

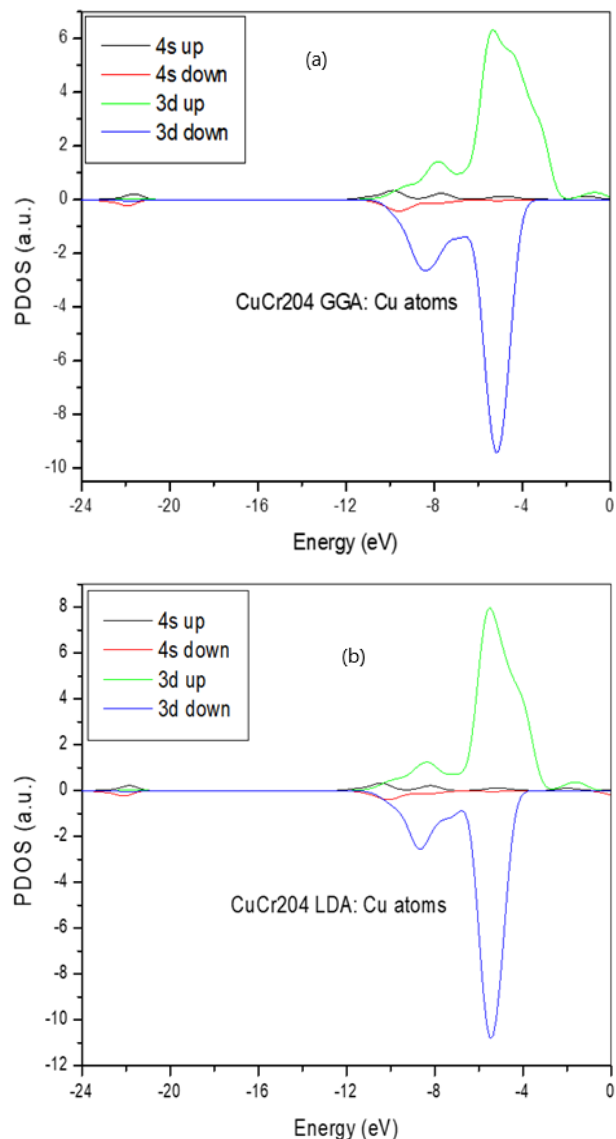


Fig. 10 – PDOS of the Cu atom calculated with (a) GGA and (b) LDA

Table 3 – Total magnetic moment for CuCr_2O_4 with I41/amd

Compound	Total magnetic moment	
	GGA-PBE	LDA-CA
CuCr_2O_4	$\mu = 2.01 \mu_B$	$\mu = 1.991 \mu_B$

The values of the magnetic moment obtained by the present calculation are slightly higher than the experimental ones [5].

On the electron density distribution map, the collection of charges between two atoms can be made by ionic and covalent bonds, it can be predicted at the atom positions according to the balance of negative and positive charges [32]. The electron density distribution map is plotted in the way of the electron density difference map, as shown in Fig. 11 along (100) crystallographic plane.

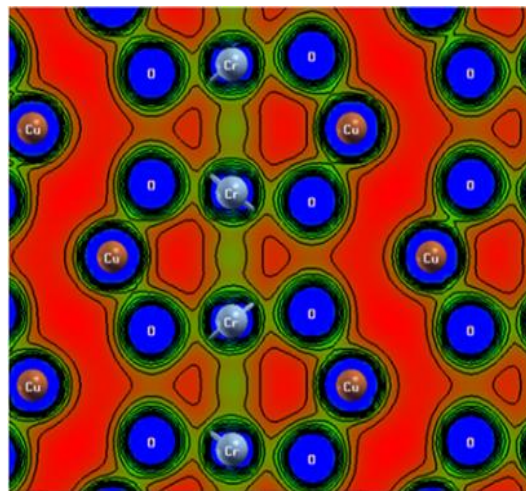


Fig. 11 – Charge density of CuCr_2O_4 for (100) plane containing both Cr–O and Cu–O bonds (GGA-PBE approximation)

From this figure, we can conclude that there exists an ionic-covalent character along the Cr–O (or Cu–O) bond. The red and blue colors indicate high and low electron densities, respectively. In the plot, the spherical charge distribution appearing around oxygen atoms denotes the ionic nature of O–O bonds. Besides, O atoms contribute highly to the DOS map (Fig. 11) where the charge distribution is maximum for O–O bonds. The ionic character describes the metallic nature of O–O bonds [29, 33]. The electronegativity appearing at Cu is relatively high in the charge density difference map because the distribution of charge around Cu is highly uniform and more charge is accumulated near Cu atoms. The covalent nature of bonds is found between Cu–Cr bonds due to the hybridization found between Cu and Cr atoms. We have also investigated the charge density difference map in different crystallographic planes and have found the same result as that found in the present investigation. The charge distributed between O and Cu atoms is very low due to interatomic distance. Further, a lower charge distribution appears in O–Cr bonds in case of interatomic distance. The preceding discussion of the charge density map shows that CuCr_2O_4 can be pictured as a highly anisotropic combination between ionic, covalent and metallic bonds.

4. CONCLUSIONS

We have carried out a detailed comprehensive study on the structural, electronic and magnetic properties of the spinel compound CuCr_2O_4 using DFT. The structural parameters of the studied compounds are calculated and compared with other studies; our results agree with experimental data. The valence and conduction bands overlap with each other at the Fermi level, indicating the metallic character of CuCr_2O_4 . Spin polarization calculations for the CuCr_2O_4 compound are performed to reveal the range of magnetic moments; spin-polarization, TDOS and DOS are calculated. In addition, spin polarization DOS shows that there is a large split between spin up and spin down channels near the Fermi level, confirming p - d hybridization. The valence and conduction bands overlap each other at the Fermi level. Our results confirm that CuCr_2O_4 has a metallic nature.

There is strong hybridization between Cu 3d and O 2p orbitals, as well as between Cr 4d and O 2p orbitals. The bonding properties indicate the ionic, covalent and metallic nature of CuCr₂O₄. The calculated total magnetic

moments are 2.01 μB (GGA-PBE) and 1.991 μB (LDA-CA). The theoretical calculated magnetic moment is slightly higher than the experimental ones.

REFERENCES

1. A.N. Yaresko, *Phys. Rev. B* **77**, 115106 (2008).
2. V. Tsurkan, H-A. Krug von Nidda, J. Deisenhofer, P. Lunkenheimer, A. Loidl, *J. Phys. Rep.* **926**, 1 (2021).
3. N. Bolandhemat, M. Rahman, A. Shuaibu, *J. Mater. Sci. Eng.* **5**, 1000250 (2016).
4. L.Q. Yan, Z.W. Jiang, X.D. Peng, L.H. He, F.W. Wang, *J. Powder Diffraction* **22** No 4, 340 (2007).
5. E. Jo, B. Kang, Ch. Kim, S. Kwon, S. Lee, *J. Phys. Rev. B* **88**, 094417 (2013).
6. A. Yaresko, V. Antonov, *J. Magn. Magn. Mater.* **310**, 1672 (2007).
7. M. Hemmida, H.-A. Krug von Nidda, Vladimir Tsurkan, A. Loidl, *J. Phys. Rev. B* **95**, 224101 (2017).
8. K. Ohgushi, Y. Okimoto, T. Ogasawara, S. Miyasaka, Y. Tokura, *J. Phys. Soc. Jpn.* **77** No 3, 034713 (2008).
9. V. Tsurkan, S. Zherlitsyn, L. Prodan, V. Felea, P. Thanh, Yurii Skourski, Zhe Wang, J. Deisenhofer, H-A Krug von Nidda, J. Wosnitzer, A. Loidl, *J. Sci. Adv.* **3**, e1601982 (2017).
10. S. Gao, O. Zaharko, V. Tsurkan, Y. Su, Jonathan S. White, G.S. Tucker, B. Roessli, F. Bourdarot, R. Sibille, D. Chernyshov, T. Fennell, Alois Loidl, C. Rüegg, *Nature Phys.* **13**, 157 (2016).
11. K. Ohgushi, Y. Okimoto, T. Ogasawara, S. Miyasaka, Y. Tokura, *J. Phys. Soc. Jpn.* **77**, 034713 (2008).
12. T. Suzuki, M. Katsumura, K. Taniguchi, T. Arima, T. Katsufuji, *Phys. Rev. Lett.* **98**, 077203 (2007).
13. S. Sarkar, T. Maitra, R. Valenti, T. Saha-Dasgupta, *Phys. Rev. Lett.* **102**, 216405 (2009).
14. S. Bordacs, D. Varjas, I. Kezsmarki, G. Mihaly, L. Baldassarre, A. Abouelsayed, C.A. Kuntscher, K. Ohgushi, Y. Tokura, *Phys. Rev. Lett.* **103**, 077205 (2009).
15. M.R. Suchomel, D.P. Shoemaker, L. Ribaud, M.C. Kemei, R. Seshadri, *Phys. Rev. B* **86**, 054406 (2012).
16. Matthew R. Suchomel, D.P. Shoemaker, Lynn Ribaud, *Phys. Rev. B* **86**, 054406 (2012).
17. B.J. Kennedy, Q. Zhou, *J. Solid State Chem.* **181**, 2227 (2008).
18. I. Efthimiopoulos, V. Tsurkan, A. Loidl, D. Zhang, Y. Wang, *J. Phys. Chem. C* **121**, 16513 (2017).
19. M. Chemurgor Kemei, *Magnetostructural and Magnetodielectric Coupling in Spinel Oxides*, PhD thesis (University of California, Santa Barbara: 2014).
20. D. Sánchez-Portal, P. Ordejón, E. Artacho, J.M. Soler, *Int. J. Quant. Chem.* **65**, 453 (1997).
21. J.M. Soler, E. Artacho, J.D. Gale, A. Garcia, J. Junquera, P. Ordejón, D. Sanchez-Portal, *J. Phys. Condens. Matter* **14**, 2745 (2002).
22. J.P. Perdew, K. Burke, M. Ernzerhof, *Phys. Rev. Lett.* **77**, 3865 (1996).
23. T. Hahn, P. Paufler, *International Tables for Crystallography, Volume A Space, Group Symmetry.* (Ed. D. Reidel) (Publishing Company Holland: Bonston, USA.: 1983).
24. A. Kokalj, *Comput. Mater. Sci.* **28**, 155 (2003).
25. R. Bencheikh, K. Belakroum, Y. Benkrima, *J. Nano-Electron. Phys.* **13** No 5, 05025 (2021).
26. N. Bolandhemat, M.Rahman, A. Shuaibu, *J. Mater. Sci. Eng.* **5**, 250 (2016).
27. L. Guo, S.T. Zhang, W.J. Feng, G. Hu, *J. Mater. Sci.* **49**, 1205 (2013).
28. D. Koller, F. Tran, P. Blaha, *Phys. Rev. B* **83**, 195134 (2011).
29. Md. Ibrahim Kholil, Md. Tofajjol Hossen Bhuiyan, *Res. Phys.* **12**, 73 (2019).
30. M. Mesbahi, M-L. Benkhedir, *U.P.B. Sci. Bull., Series A* **79**, 1223 (2017).
31. U. Shankar Sharma, R. Shah, *AIP Conf. Proc.* **1953**, 030091 (2018).
32. *High-Resolution Imaging and Spectrometry of Materials* (Eds by F. Ernst, M. Ruhle) (Springer-Verlag: Berlin Heidelberg, New York: 2003).
33. R.P. Singh, *J. Magnesium Alloy.* **2**, 349 (2014).

Теоретичне дослідження шпінельної структури CuCr₂O₄ в тетрагональній фазі з використанням теорії функціоналу густини

Radia Bencheikh, Karima Belakroum

Université Kasdi Merbah-Ouargla, Faculté des Mathématiques et des Sciences de la Matière, Département de physique, route de Ghardaïa 30000, Alegria

Ми представляємо детальне теоретичне дослідження потрійних оксидів шпінелі CuCr₂O₄ з тетрагональною структурою I4₁/amd за допомогою теорії функціоналу густини (DFT). Розрахунки були виконані з використанням двох наближень до DFT, а саме наближення локальної щільності (LDA) і наближення узагальненого градієнта (GGA), обидва в спин-поляризованій версії. Для LDA ми використовували обмінно-кореляційний потенціал Ceperley-Alder, тоді як для розрахунків GGA ми використовували схему Perdew-Burke-Ernzerhof (PBE). Ми оптимізували кристалічні структури за допомогою методу плоскої хвилі псевдопотенціалу та проаналізували на основі густини станів (DOS), парціальної густини станів (PDOS) та електронної зонної структури. Дійсно, це корисний метод прогнозування кристалічних структур CuCr₂O₄. PDOS Cu, Cr та O показала, що катіон Cr є домінуючим джерелом для вивчення магнітних властивостей CuCr₂O₄. Розрахунки спінової поляризації, виконані для CuCr₂O₄, і DOS показують, що існує велике спінове розщеплення між каналами зі спінами вгору та вниз поблизу рівня Фермі, що підтверджує *p-d* гібридизацію. Теоретично розрахований магнітний момент трохи перевищує експериментальні результати. Зроблено висновок, що оптимізований параметр решітки для GGA набагато краще узгоджується з експериментальними результатами, ніж для LDA. Валентна зона та зона провідності перекривали одна одну на рівні Фермі, що вказує на металеву природу CuCr₂O₄.

Карти різниці густини заряду показують, що зв'язки Cu–Cr міцніші, ніж зв'язки Cu–O. Отримані результати порівняли з експериментальними значеннями та виявили гарне узгодження з ними. Результати даного дослідження можуть бути використані в майбутньому аналізі термодинамічних, оптичних і пружних властивостей цієї сполуки.

Ключові слова: CuCr_2O_4 , структура шпінелі, Теорія функціоналу густини (DFT), Електронна зонна структура, Магнітні властивості.